解　　説

~~Review on~~ Crystallographic Lamellar Texture Formation and Enhanced Mechanical Properties via Lamellar Interface in Ni-based Inconel 718 Fabricated by Laser Powder Bed Fusion

Ozkan GOKCEKAYA*, **, Takuya ISIMOTO**, *** and Takayoshi NAKANO*, **

（Received 16 March 2023, Accepted 15 May 2023）

Metallic materials are fundamental to a vast majority of industries. Although the understanding of the strengthening and microstructure relation of metals and alloys has matured, additive manufacturing of metallic materials is expanding the possibilities of obtaining unique microstructural characteristics and enhanced mechanical properties. In this review, the microstructure control of the crystallographic texture and grain morphology and its effect on the strengthening of Inconel 718, a major Ni-based superalloy fabricated by laser powder bed fusion (LPBF), is discussed in terms of characteristics that are unique to the manufacturing method. In particular, this review focuses on the unique crystallographic lamellar microstructure, which can only be formed by the LPBF method, and its enhancement by the effect of the lamellar microstructure interfaces.

Key Words: Laser Powder Bed Fusion, Inconel 718, Texture, Crystallographic Lamellae, Strengthening

1. Introduction

Ni-based superalloys have been widely used in the aerospace, automotive, and energy industries because of their excellent creep resistance, high yield strength, and good weldability[1), 2)]. Ni-based superalloy parts, particularly for aerospace applications, are designed to have a complex shape that requires high-precision fabrication; however, traditional manufacturing processes are time-consuming and expensive to satisfy industrial expectations[3), 4)]. For example, turbine blades, as thin-wall structures comprised of single-crystal Ni-based alloys with complex internal cooling channels, are challenging to fabricate using traditional methods. In recent years, tremendous progress has been made in adapting additive manufacturing (AM) techniques to fabricate high-density and near-net-shape components in various industries. Laser powder bed fusion (LPBF), a well-established AM technique, provides a cost-effective and time-efficient way to fabricate parts with complicated geometries and has become an important candidate for fabricating complex Ni-based alloy parts. In contrast to the Ni-based alloy parts fabricated by conventional methods[5), 6)], those fabricated by LPBF exhibit microstructure characteristics resembling the directional solidification process owing to the rapid melting and solidification process.

Inconel 718 (IN718), one of the most common Ni-based superalloys, has been preferred in the nuclear energy and petroleum industries, aircraft engine applications, and many other applications that require good corrosion and creep resistance, high strength, and long fatigue life at high temperatures. Therefore, the control and enhancement of the mechanical properties of IN718 are key initiatives in the environmental and energy industries to reduce CO_2 emissions.

According to the literature, a well-established LPBF process displays dominant <100> columnar grain formation for IN718 parts along the build direction because of layer-by-layer manufacturing[7)]. Moreover, understanding the effect of the LPBF process parameters on the thermal characteristics of the fabrication process, such as the heat flow direction, thermal gradient, solidification rate, and resulting melt pool shape, can be utilized to control the grain morphology and crystallographic texture formation[8)].

Although AM processing of metals and alloys has been extensively studied in the past decade, IN718 with a single-crystal-like microstructure has recently been reported[9)]. In this study, a unique microstructure development with lamellar formation was achieved, which is peculiar to the AM method. IN718 is a precipitation-strengthened superalloy with multiple strengthening mechanisms such as solution strengthening, grain boundary strengthening, and precipitation strengthening. However, the strengthening mechanisms that can be enhanced by LPBF processing are not yet known.

This article aims to elaborate on the significant findings of a recent study[9)] overcoming the trade-off between the strength and

＊ Division of Materials and Manufacturing Science, Graduate School of Engineering, Osaka University (2-1 Yamada-Oka, Suita, Osaka 565-0871, Japan)
＊＊ Anisotropic Design & Additive Manufacturing Research Center, Osaka University (2-1 Yamada-Oka, Suita, Osaka 565-0871, Japan)
＊＊＊ Aluminium Research Center, School of Sustainable Design, University of Toyama (3190 Gofuku, Toyama, Toyama 930-8555, Japan)

ductility of IN718 through crystallographic texture control and grain orientation.

2. Crystallographic texture control

Various industrial applications require resistance to high-temperature environments while maintaining good strength, creep resistance, corrosion resistance, and a long fatigue life[3]. As a general approach to satisfy these expectations, the major focus is on discovering new alloy compositions[10]. However, with a better understanding of the AM process, recent studies have focused on realizing the unique properties of additively manufactured metallic materials[5, 9-12]. From this perspective, IN718 parts fabricated by LPBF were investigated in terms of microstructure differences owing to the LPBF process parameters[9]. The recently published study on the fabrication of IN718 by LPBF reported tunable microstructural characteristics with unique crystallographic texture formations and enhanced mechanical properties[9].

Scanning electron microscopy (SEM) micrographs and inverse pole figure (IPF) maps with the corresponding pole figures of three distinct textures of IN718 were recorded in the same region, as shown in **Fig. 1**. We note that lack of fusion, cracks, and voids are observed as common defects owing to insufficient laser energy, high cooling rate, and/or instability of the melt pool of the LPBF process[11, 12]. However, highly dense IN718 specimens with no significant voids or defects are successfully fabricated by LPBF, as shown in the cross-sectional SEM images. These three distinct crystallographic textures were identified as crystallographic lamellar (CLM), single-crystal (SCM), and polycrystal (PCM) microstructures, and evaluated to clarify the texture formation mechanism and its effect on the mechanical properties of IN718 fabricated by LPBF. The formation of the cellular microstructure was observed throughout the cross-section, as shown in **Fig. 1**. As indicated by the arrows showing the <100> cell growth directions, the texture formation of the SCM part followed the development of <100>-oriented cells in each half of the melt pool with ±45° to the build direction, which produced a <110> single-crystal-like cubic texture in the build direction. In contrast to SCM, in CLM, <100>-oriented cells grew from the bottom of the melt pool, forming a lamellar <100> texture at the center of the melt pool. For the PCM, the cell orientation was random, thus weakening the texture.

To understand the relationship between the microstructure developed in the underlying and adjacent melt pools and the subsequent crystallographic orientation of the grains, understanding the solid/liquid interface related to the thermal gradient (G) and the migration velocity of the solid/liquid interface (R)[13, 14] is necessary. The thermal diffusion analysis of IN718 processed by a laser source was conducted by finite element analysis, and the temperature distribution inside the melt pool and melt pool shape according to the thermal distribution were investigated, as shown in **Fig. 2**. The numerical simulations of the thermal characteristics of the melt pool in the published work showed good agreement with the microstructural observations, indicating a decrease in G/R value from CLM to SCM and further decrease to PCM. Notably, the decrease in G/R indicates the sequential formation of planar, cellular, columnar dendritic, and equiaxed dendritic structures. However, the unique lamellar microstructure differed from that of the SCM and was further investigated in terms of the melt pool shape and thermal gradient direction.

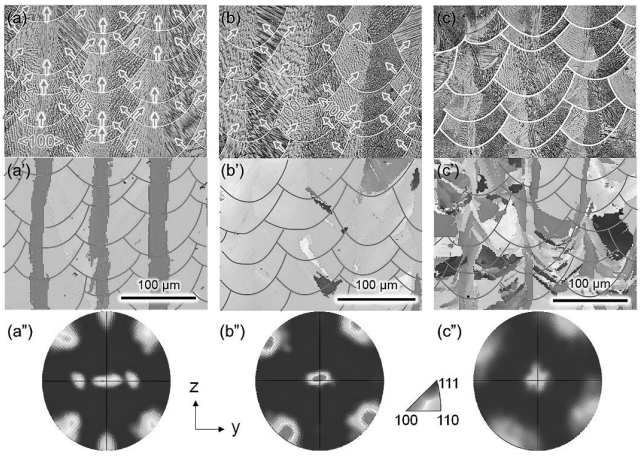

Fig. 1 Microscopic images (a-c) and IPF maps (a'-c') with corresponding pole figures (a"-c") of CLM (a), SCM (b), and PCM (c) specimens in the same region. Modified from reference[9] (published under CC BY 4.0 license). (For interpretation of the references to color in this figure, the reader is referred to the web version of this article.)

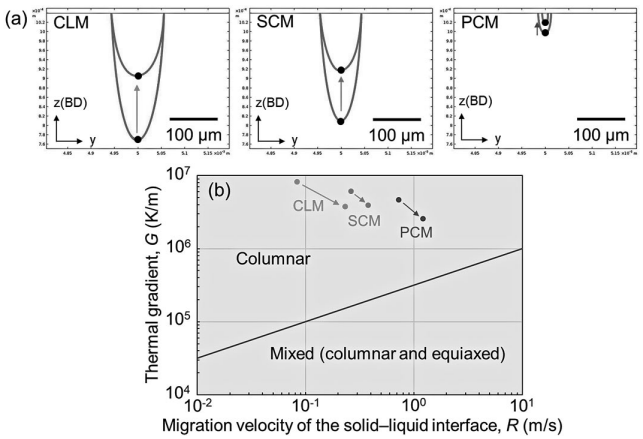

Fig. 2 (a) Liquid-solid interface at the time when the melt pool depth recorded its maximum and the half of the maximum, and (b) the simulated R and G plotted on the solidification map of IN718. Modified from reference[9] (published under CC BY 4.0 license).

For this purpose, the top layers of the CLM and SCM parts that were not affected by the thermal cycling of the LPBF process were analyzed, and the results are shown in **Fig. 3**. In the case of the CLM, a deeper and wider melt pool shape was observed, which resulted in a small curvature at the bottom of the melt pool and a strongly oriented heat flow direction along the build direction. These LPBF-specific properties promote lamellar formation at the center of each melt pool, thus forming a unique microstructure with enhanced mechanical properties. The alignment of heat flow in the SCM fabrication condition showed inconsistency compared to the CLM; therefore, only cell growth with a ±45° orientation was detected, forming a single-crystal-like microstructure.

The unique microstructural characteristics of IN718 fabricated by LPBF exhibited a significant improvement in the mechanical strength of the parts, which can be related to various strengthening mechanisms. Moreover, texture-induced strengthening and the effect of texture on the common strengthening mechanisms are discussed in the next chapter.

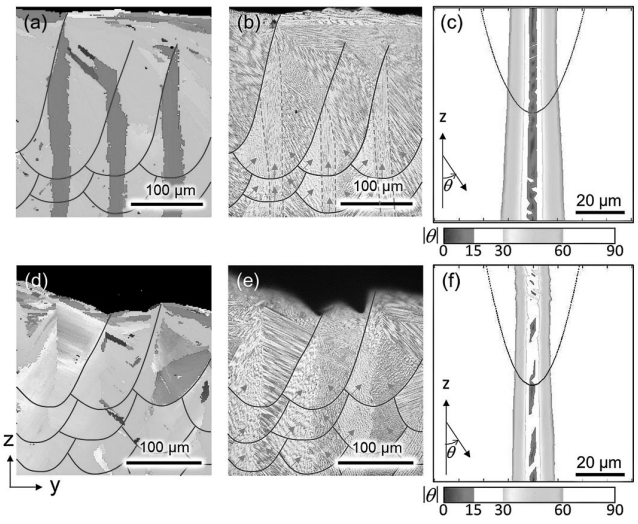

Fig. 3 IPF maps (a, d) and SEM micrographs (b, e) of CLM and SCM with the angle of heat flow direction for CLM (c) and SCM (f). Modified from reference [9] (published under CC BY 4.0 license). (For interpretation of the references to color in this figure, the reader is referred to the web version of this article.)

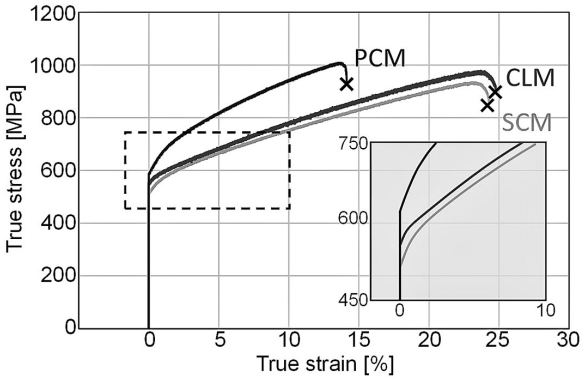

Fig. 4 Tensile engineering stress-strain curves of CLM, SCM, and PCM specimens. Modified from reference[9] (published under CC BY 4.0 license).

3. Enhanced mechanical properties

For Ni-based superalloys, γ′ phase formation is considered the primary strengthening mechanism. However, IN718 parts fabricated by LPBF lacked γ′ phase formation owing to the fast-cooling rate of the LPBF process. Although LPBF-fabricated IN718 was nearly a single γ phase, it reached approximately 800 MPa yield and 1300 MPa ultimate tensile strength (UTS) without γ′ phase formation, which was higher than that reported in previous studies and standard Cast-IN718[5), 15), 16)]. The effect of the texture on the strength of IN718 is shown in **Fig. 4**. CLM and SCM exhibited better elongation than PCM owing to their single-crystal-like microstructural characteristics. However, the PCM exhibited a higher yield strength owing to its smaller grain size, as shown in **Fig. 1**. Notably, CLM outperformed SCM in terms of yield strength, UTS, and elongation, addressing the strength-ductility trade-off, which has been a long-standing challenge in materials science.

The major mechanisms for the enhanced strength and ductility of the CLM were attributed to a smaller stress transfer coefficient between major <110> and lamella <100> grains[17)] and the alignment of grain boundaries according to the tensile direction compared to the SCM parts. The stress transfer coefficient (N_{ij}) is expressed using the following equation[17)]:

$$P_j^B = P_i^A \cdot N_{ij} = P_i^A \cdot [(e_i^A \cdot e_j^B)(g_i^A \cdot g_j^B) + (e_i^A \cdot g_j^B)(e_j^B \cdot g_j^A)],$$

where P_i^A and P_i^B indicate the shear stress values of crystals A and B, respectively (**Fig. 5**). Therefore, the smaller the N_{ij}, the more stress is required for dislocations to transmit to the interface, increasing the strength. Although the N_{ij} of a single

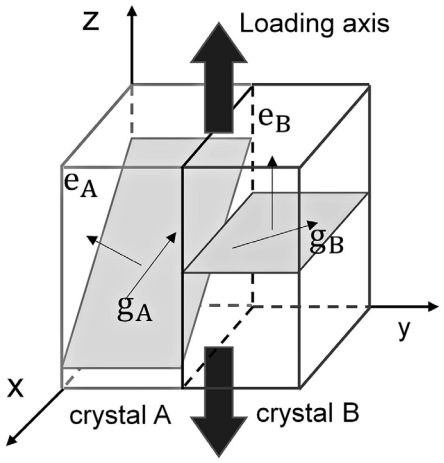

Fig. 5 Bicrystalline tensile specimen with longitudinal boundary. Modified from reference[9] (published under CC BY 4.0 license).

crystal is equal to one, CLM's is 0.819, indicating texture-induced resistance to dislocation transfer between the <110> grains and <100> grains[18]. Therefore, the CLM exhibited a higher strength than the SCM parts. The advantage of LPBF is that it promotes unique microstructural characteristics achieved through layer-by-layer fabrication, resulting in causing epitaxial growth along the build direction and additional strengthening mechanisms. This information can be applied to other LPBF-fabricated metals to improve their mechanical properties.

A significant increase in the elongation of CLM compared to SCM was discussed considering its grain boundary alignment with the tensile direction because anisotropy is a common property of additively manufactured materials[19]. As shown in **Fig. 1**, the <100> lamella grains developed along the build direction, which was parallel to the tensile load direction. However, grains with varied crystal orientations and sizes in the SCM were detected, which were formed owing to local instabilities of the melt pool, forming grain boundaries with various angles in the tensile direction. Notably, when comparing the CLM and SCM, perpendicular grain boundaries according to tensile load are prone to mode I crack formation[20]. Although CLM with mainly parallel grain boundaries along the tensile load resisted crack initiation/propagation, SCM grains with vertically aligned grains along the tensile direction were weak for crack formation; therefore, better elongation was achieved with CLM.

The concept of strengthening the CLM by decreasing the stress transfer coefficient was further investigated by mechanical anisotropy, which was performed by tilting the fabrication direction to 35° and 45°, as shown in **Fig. 6**. Owing to the tilt angle of the LPBF fabrication, the crystallographic texture characteristic of the CLM could be altered, as shown in **Fig. 6**. This strategy resulted in a decrease in the stress transfer coefficient to a lower value (0.652) than that of CLM-0° (0.819). Owing to the lower stress transfer coefficient, CLM-35° exhibited higher strength than CLM-0° (**Fig. 7**), despite consisting of a higher average grain size (32.5 μm) than CLM-0° (24.2 μm), which contradicts the Hall-Petch strengthening[21]. However, the tilted fabrication caused perpendicular grain boundaries in CLM-0° and CLM-45°, which can be observed from the IPF maps in **Fig. 6**; therefore, the resulting decrease in elongation was because of easier crack initiation/propagation via mode I opening, as indicated previously.

AM has been proven to form unique microstructures and enhance mechanical properties, which are not possible using traditional manufacturing methods. By utilizing microstructure control and distinctive texture formation by the LPBF process, the strength-ductility trade-off for metals was addressed for IN718, and this approach can be applied to various other metal materials.

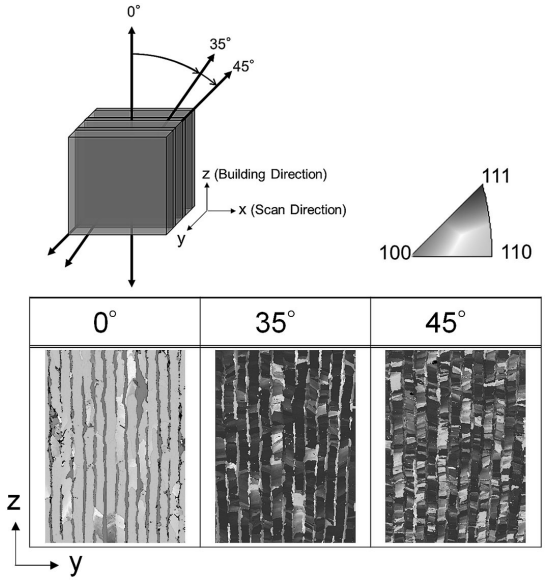

Fig. 6 Schematic presentation of CLM for 0°, 35°, and 45° tilted from build direction. IPF maps (a) showing the variation in crystallographic orientation parallel to the tensile direction. Modified from reference[9] (published under CC BY 4.0 license). (For interpretation of the references to color in this figure, the reader is referred to the web version of this article.)

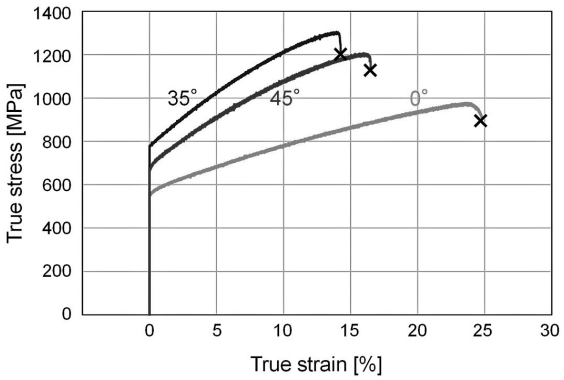

Fig. 7 Tensile engineering stress-strain curves of CLM-0°, CLM-35°, and CLM-45°. Modified from reference[9] (published under CC BY 4.0 license).

4. Outlook

The requirement for the structural and functional properties of engineering materials is increasing with the advancement of technology. Most research on improving the properties of metallic materials has focused on compositional design. However, a recent study[9] on IN718 fabricated by LPBF demonstrated that the microstructural characteristics of IN718 could be tuned to achieve lamellar, single-crystal, and polycrystalline microstructures. The CLM is distinctive to the LPBF process, displaying <110> major and <100> lamellar grains along the build direction. The mechanical properties of the CLM are enhanced owing to its anisotropy in grain formation and a decrease in the stress transfer

coefficient. This recent study proved a new approach to address the strength-ductility trade-off dilemma, which can be applied to other metallic materials.

Acknowledgments

This work was supported by CREST-Nanomechanics: Elucidation of macroscale mechanical properties based on understanding nanoscale dynamics for innovative mechanical materials (Grant Number: JPMJCR2194) from the Japan Science and Technology Agency (JST).

References

1) Q. Jia and D. Gu: “Selective laser melting additive manufacturing of Inconel 718 superalloy parts: Densification, microstructure and properties”, J. Alloys Compd. **585** (2014), 713–721.
2) T. DebRoy, H.L. Wei, J.S. Zuback, T. Mukherjee, J.W. Elmer, J.O. Milewski, A.M. Beese, A. Wilson-Heid, A. De and W. Zhang: “Additive manufacturing of metallic components – Process, structure and properties”, Prog. Mater. Sci. **92** (2018), 112–224.
3) T.S. Srivatsan and T.S. Sudarshan: “Additive Manufacturing: Innovations, Advances, and Applications”, CRC Press, 2015. https://books.google.co.jp/books?id=dXm9CgAAQBAJ.
4) D. Herzog, V. Seyda, E. Wycisk and C. Emmelmann: “Additive manufacturing of metals”, Acta Mater. **117** (2016), 371–392.
5) V.A. Popovich, E. V Borisov, A.A. Popovich, V.S. Sufiiarov, D. V Masaylo and L. Alzina: “ Functionally graded Inconel 718 processed by additive manufacturing: Crystallographic texture, anisotropy of microstructure and mechanical properties”, Mater. Des. **114** (2017), 441–449.
6) H.L. Wei, J. Mazumder and T. DebRoy: “Evolution of solidification texture during additive manufacturing”, Sci. Rep. **5** (2015), 16446.
7) H.Y. Wan, Z.J. Zhou, C.P. Li, G.F. Chen and G.P. Zhang: “ Effect of scanning strategy on mechanical properties of selective laser melted Inconel 718”, Mater. Sci. Eng. A. **753** (2019), 42–48.
8) N. Raghavan, R. Dehoff, S. Pannala, S. Simunovic, M. Kirka, J. Turner, N. Carlson and S.S. Babu: “Numerical modeling of heat-transfer and the influence of process parameters on tailoring the grain morphology of IN718 in electron beam additive manufacturing”, Acta Mater. **112** (2016), 303–314.
9) O. Gokcekaya, T. Ishimoto, S. Hibino, J. Yasutomi, T. Narushima and T. Nakano: “ Unique crystallographic texture formation in Inconel 718 by laser powder bed fusion and its effect on mechanical anisotropy”, Acta Mater. **212** (2021), 116876.
10) O. Gokcekaya, T. Ishimoto, Y. Nishikawa, Y.S. Kim, A. Matsugaki, R. Ozasa, M. Weinmann, C. Schnitter, M. Stenzel, H.S. Kim, Y. Miyabayashi and T. Nakano: “ Novel single crystalline-like non-equiatomic TiZrHfNbTaMo bio-high entropy alloy (BioHEA) developed by laser powder bed fusion”, Mater. Res. Lett. **11** (2023), 274–280.
11) O. Gokcekaya, N. Hayashi, T. Ishimoto, K. Ueda, T. Narushima and T. Nakano: “ Crystallographic orientation control of pure chromium via laser powder bed fusion and improved high temperature oxidation resistance”, Addit. Manuf. **36** (2020), 101624.
12) O. Gokcekaya, T. Ishimoto, T. Todo, P. Wang and T. Nakano: “Influence of powder characteristics on densification via crystallographic texture formation: Pure tungsten prepared by laser powder bed fusion”, Addit. Manuf. Lett. **1** (2021), 100016.
13) S. Bontha, N.W. Klingbeil, P.A. Kobryn and H.L. Fraser: “Effects of process variables and size-scale on solidification microstructure in beam-based fabrication of bulky 3D structures”, Mater. Sci. Eng. A. **513–514** (2009), 311–318.
14) P. Promoppatum, S.-C. Yao, P.C. Pistorius and A.D. Rollett: “A Comprehensive Comparison of the Analytical and Numerical Prediction of the Thermal History and Solidification Microstructure of Inconel 718 Products Made by Laser Powder-Bed Fusion”, Engineering. **3** (2017), 685–694.
15) M.E. Aydinöz, F. Brenne, M. Schaper, C. Schaak, W. Tillmann, J. Nellesen and T. Niendorf: “On the microstructural and mechanical properties of post-treated additively manufactured Inconel 718 superalloy under quasi-static and cyclic loading”, Mater. Sci. Eng. A. **669** (2016), 246–258.
16) E. Chlebus, K. Gruber, B. Kuźnicka, J. Kurzac and T. Kurzynowski: “Effect of heat treatment on the microstructure and mechanical properties of Inconel 718 processed by selective laser melting”, Mater. Sci. Eng. A. **639** (2015), 647–655.
17) J.D. Livingston and B. Chalmers: “Multiple slip in bicrystal deformation”, Acta Metall. **5** (1957), 322–327.
18) N. V Malyar, G. Dehm and C. Kirchlechner: “Strain rate dependence of the slip transfer through a penetrable high angle grain boundary in copper”, Scr. Mater. **138** (2017), 88–91.
19) S. Hibino, T. Todo, T. Ishimoto, O. Gokcekaya, Y. Koizumi, K. Igashira and T. Nakano: “Control of crystallographic texture and mechanical properties of Hastelloy-X via laser powder bed fusion”, Crystals. **11** (2021), 1064.
20) M. Ni, C. Chen, X. Wang, P. Wang, R. Li, X. Zhang and K. Zhou: “Anisotropic tensile behavior of in situ precipitation strengthened Inconel 718 fabricated by additive manufacturing”, Mater. Sci. Eng. A. **701** (2017), 344–351.
21) S. Ghorbanpour, M.E. Alam, N.C. Ferreri, A. Kumar, B.A. McWilliams, S.C. Vogel, J. Bicknell, I.J. Beyerlein and M. Knezevic: “Experimental characterization and crystal plasticity modeling of anisotropy, tension-compression asymmetry, and texture evolution of additively manufactured Inconel 718 at room and elevated temperatures”, Int. J. Plast. **125** (2020), 63–79.

Mail Address

Takayoshi NAKANO　nakano@mat.eng.osaka-u.ac.jp